Electronic Supplementary Information

Hierarchical Co_3O_4@Au-decorated PPy core/shell nanowire arrays: an efficient integration of active materials for energy storage

Wei Hong,[ab] Jinqing Wang,*[a] Zhangpeng Li,[a] and Shengrong Yang *[a]

[a] State Key Laboratory of Solid Lubrication, Lanzhou Institute of Chemical Physics,

Chinese Academy of Sciences, Lanzhou, 730000, P. R. China

[b] University of Chinese Academy of Sciences, Beijing, 100080, P. R. China

---

∗ Corresponding authors: E-mail: jqwang@licp.cas.cn; sryang@licp.cas.cn
Fax: +86 931 8277088; Tel: +86 931 4968076

1. Experimental sections

1.1 Synthesis of Co_3O_4 nanowire arrays

The Co_3O_4 nanowire arrays (Co_3O_4 NWAs) was synthesized by a simple hydrothermal method, and similar synthesis process can be found in the previous reports.[1-3] Typically, the reaction solution was obtained by mixing $Co(NO_3)_2 \cdot 6H_2O$ (1.5 mmol), NH_4F (3 mmol) and urea (7.5 mmol) in 50 mL of ultrapure water. After string for 1 h, the homogeneous pink solution was transferred into a Teflon-lined stainless steel autoclave. A piece of Ni foam was immersed into the reaction solution. Subsequently, the bottle was capped and maintained at 120 °C for 8 h in an electric oven and then cooled down to room temperature. After the reaction, the sample was collected and rinsed several times with ultrapure water. Finally, the Co_3O_4 NWAs was obtained by annealing at 300 °C for 3 h with a heating rate of 2 °C min^{-1}.

1.2 Construction of hybrid Co_3O_4@Au-decorated PPy core/shell nanowire arrays

The hybrid Co_3O_4@Au-decorated PPy core/shell nanowire arrays (Co@Au-PPy NWAs) was synthesized by a modified technique according to the previous reports.[4, 5] In detail, 0.1 mL pyrrole monomer was added into 30 mL ethanol with vigorous stirring for 10 min. After that, a piece of the obtained Co_3O_4 NWAs was placed in a clean petri dish. The aforementioned pyrrole ethanol solution was slowly dropped into the sample. Then, the Co_3O_4 NWAs having absorbed the pyrrole monomers was dipped into $HAuCl_4$ aqueous solution, and left in dark overnight before rinsing with ultrapure water and ethanol.

1.3 Preparation of Co_3O_4@PPy core/shell nanowire arrays

For the synthesis of Co_3O_4@PPy core/shell nanowire arrays, the self-supported Co_3O_4 NWAs was directly used as backbone for the growth of PPy layer by electro-deposition.[6, 7] Briefly, the electro-deposition was conducted by a CHI 660E electrochemical workstation with a standard three-electrode glass cell at room temperature. The reaction solution for electro-polymerization was obtained by mixing pyrrole (50 mM), $LiClO_4$ (40 mM) and SDS (56 mM) in 100 mL ultrapure water. The deposition of PPy layer was carried out at 0.8 V (vs. Ag/AgCl) for 60 s, 90 s and 120 s, respectively.

1.4 Materials characterization

X-ray diffraction (XRD) patterns were recorded by a Rigaku XRD-2400 diffractometer, using Cu-Kα radiation at 40 kV and 60 mA. The nanostructured samples were analyzed using a field emission scanning electron microscope (FESEM, JSM-6701F) and a field emission transmission electron microscope (FETEM, TF20) with an energy-dispersive X-ray spectroscopy (EDX) analyzer. X-ray photoelectron spectroscopy (XPS) was carried out by using ESCALAB 210 spectrometer (VG Scientific, UK).

The electrochemical measurements were carried out in a three-electrode electrochemical cell using the CHI 660E Electrochemical Workstation at room temperature with the 2 M NaOH as the electrolyte. The Ni foam supported active materials (Co_3O_4 mass ≈ 2.0 mg cm^{-2}, Co_3O_4@PPy ≈ 3.0 mg cm^{-2}, Co_3O_4@Au-PPy mass ≈ 3.1 mg cm^{-2}) were used directly as the working electrode. A Pt plate and an SCE electrode were used as the counter electrode and the reference electrode, respectively. Electrochemical impedance spectroscopy (EIS) tests were conducted by using a perturbation amplitude of 5 mV in the frequency range from 0.01 Hz to 100 kHz. The mass-specific capacitance (MSC, Cs) [F g^{-1}] and areal-specific capacitance (ASC, Ca) [F cm^{-2}] were calculated from the galvanostatic discharge curves using equations as below:

$$Cs = It/m\Delta V$$

$$Ca = It/S\Delta V$$

where I represents the charge-discharge current (A), t is the discharge time (s), ΔV is the potential (V), S is the geometrical area of the electrode, and m designates the total mass of the active materials (g).[1, 4, 8]

1.5 Fabrication of an aqueous asymmetric supercapacitor

To fabricate an aqueous asymmetric supercapacitor, the synthesized Co_3O_4@Au-PPy on Ni foam was directly used as positive electrode, and the activated carbon (AC) was used as negative electrode. The electrochemical performances of asymmetric supercapacitor (AS) were explored under a two-electrode cell in 2 M NaOH electrolyte solution.[9] The negative electrode was prepared by a traditional "slurry-coating" method.[6] The charge balance between the two electrodes will follow the relationship $q^+ = q^-$. The charge stored (q) by each electrode depends on the equation:

$$q = mC\Delta V$$

where C represents the specific capacitance of the electrode (F g^{-1}), ΔV is the potential (V), and m designates the total mass of the active materials (g). To get $q^+ = q^-$, the mass ratio between the positive and negative electrodes needs to follow:

$$m_{+}/m_{-} = \Delta V_{-}\,C_{-}/\Delta V_{+}\,C_{+}$$

The energy density (E) and power density (P) were also calculated as follows:[8, 10]

$$E = 0.5\,C(\Delta V)^2$$

$$P = E/t$$

2. Supplementary Figures

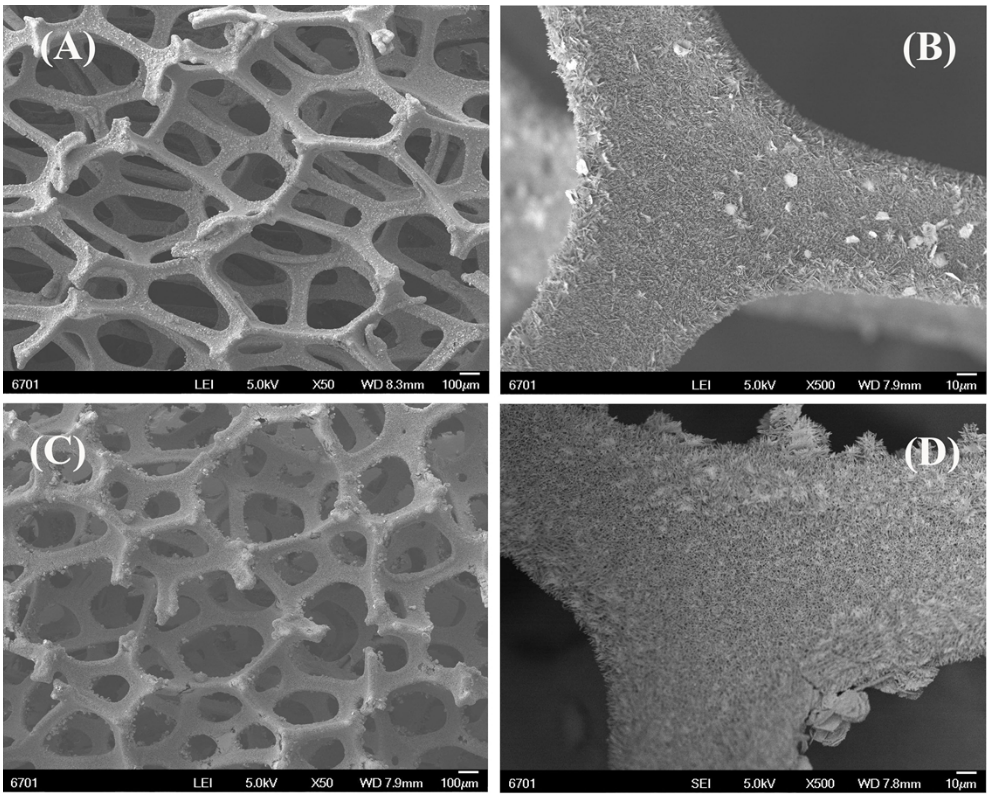

Fig. S1 SEM images of the bare Co_3O_4 NWAs (A, B) and hybrid Co_3O_4@Au-PPy NWAs (C, D) electrodes with different magnification times. Scale bar: 100 μm for A, C; and 10 μm for C, D.

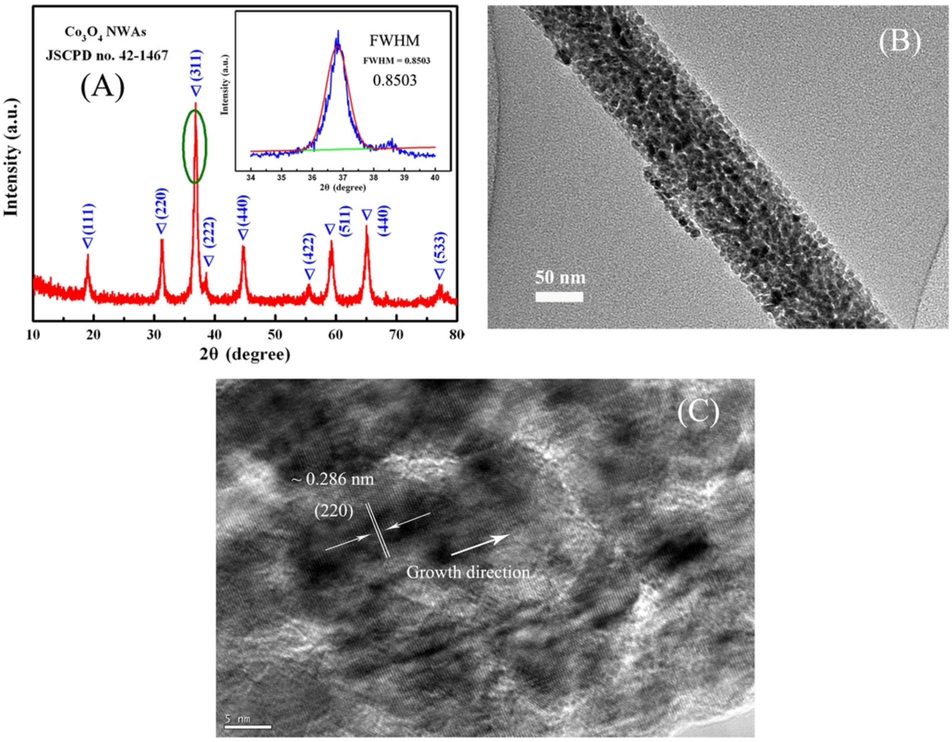

Fig. S2 (A) XRD patterns, (B) TEM and (C) HRTEM images of the bare Co_3O_4 NWAs scraped from Ni foam substrate. The inset shows the highest intensity peak of the as-synthesized sample.

Based on the XRD patterns, the average crystallite size of the bare Co_3O_4 NWAs can be calculated using the Scherrer equation as below:

$$D = \frac{k\,\lambda}{B\cos\theta}$$

In our case, the calculated crystallite size of the bare Co_3O_4 NWAs is ~ 9.7 nm, which is in good agreement with the TEM observation. As can be seen from **Fig. S2 B**, the individual Co_3O_4 nanowire consists of numerous small nanoparticles with average diameter of ~ 10 nm and a large quantity of mesoporous structures. The novel structural features can be generally explained by the successive release of H_2O and gases during the thermal annealing.

Fig. S2 C shows the HRTEM image of the bare Co_3O_4. The interplanar spacing is about 0.286 nm, which corresponds to the (220) plane of the cubic crystalline Co_3O_4, indicating the growth plane of the nanowires is along the (220) planes. This is similar to the result reported by Xia *et al*.[3b]

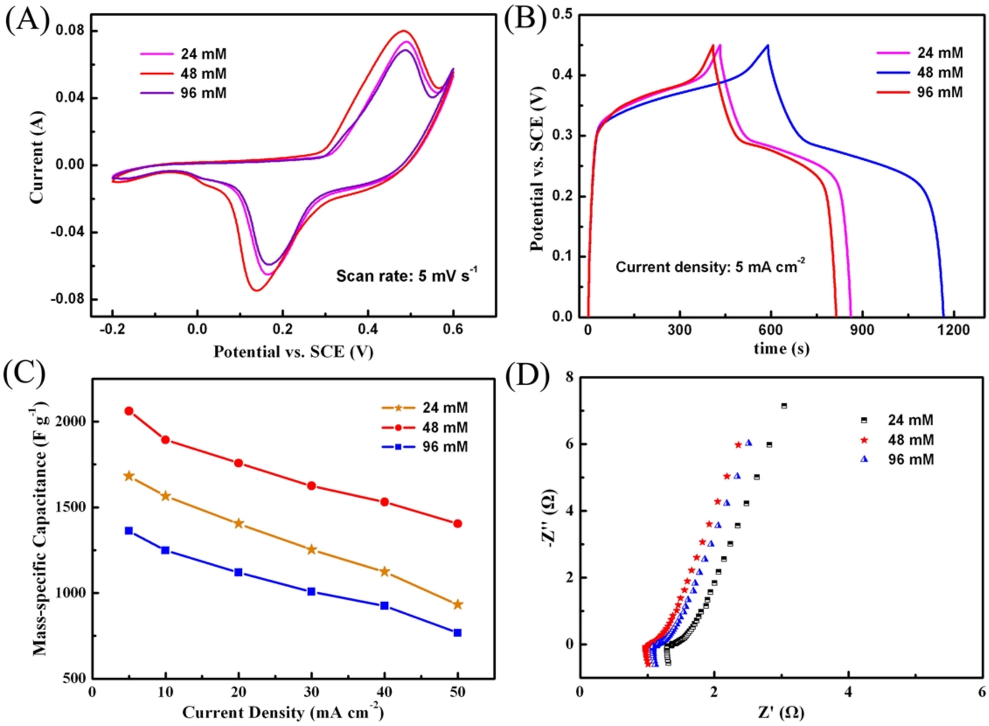

Fig. S3 (A) CV curves of hybrid Co_3O_4@Au-PPy electrodes at a scan rate of 5 mV s^{-1}, (B) Charge-discharge curves of hybrid Co_3O_4@Au-PPy electrodes at a different current density of 5 mA cm^{-2}, (C) The specific capacitance values of hybrid Co_3O_4@Au-PPy electrodes as a function of current density, (D) EIS tests with the frequency from 0.01 Hz to 100 kHz.

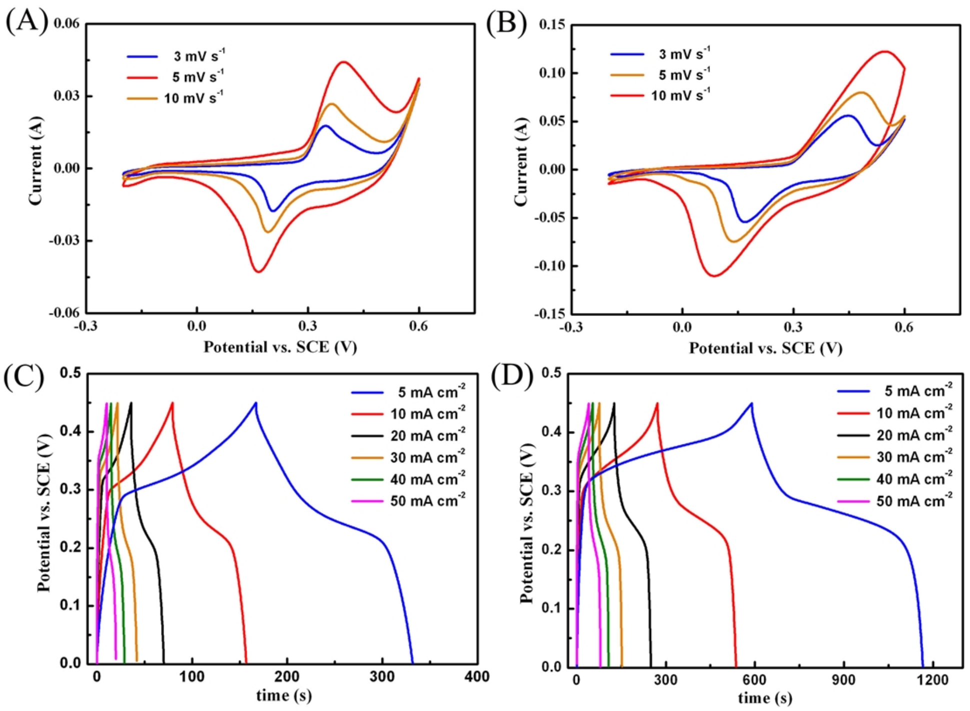

Fig. S4 Electrochemical performances of the bare Co_3O_4 NWAs and hybrid Co_3O_4@Au-PPy NWAs electrodes measured in 2 M NaOH. (A, B) CV curves of the bare Co_3O_4 NWAs and hybrid Co_3O_4@Au-PPy NWAs electrodes at different scan rates, (C, D) Charge/discharge curves of the bare Co_3O_4 NWAs and hybrid Co_3O_4@Au-PPy NWAs electrodes at different current densities.

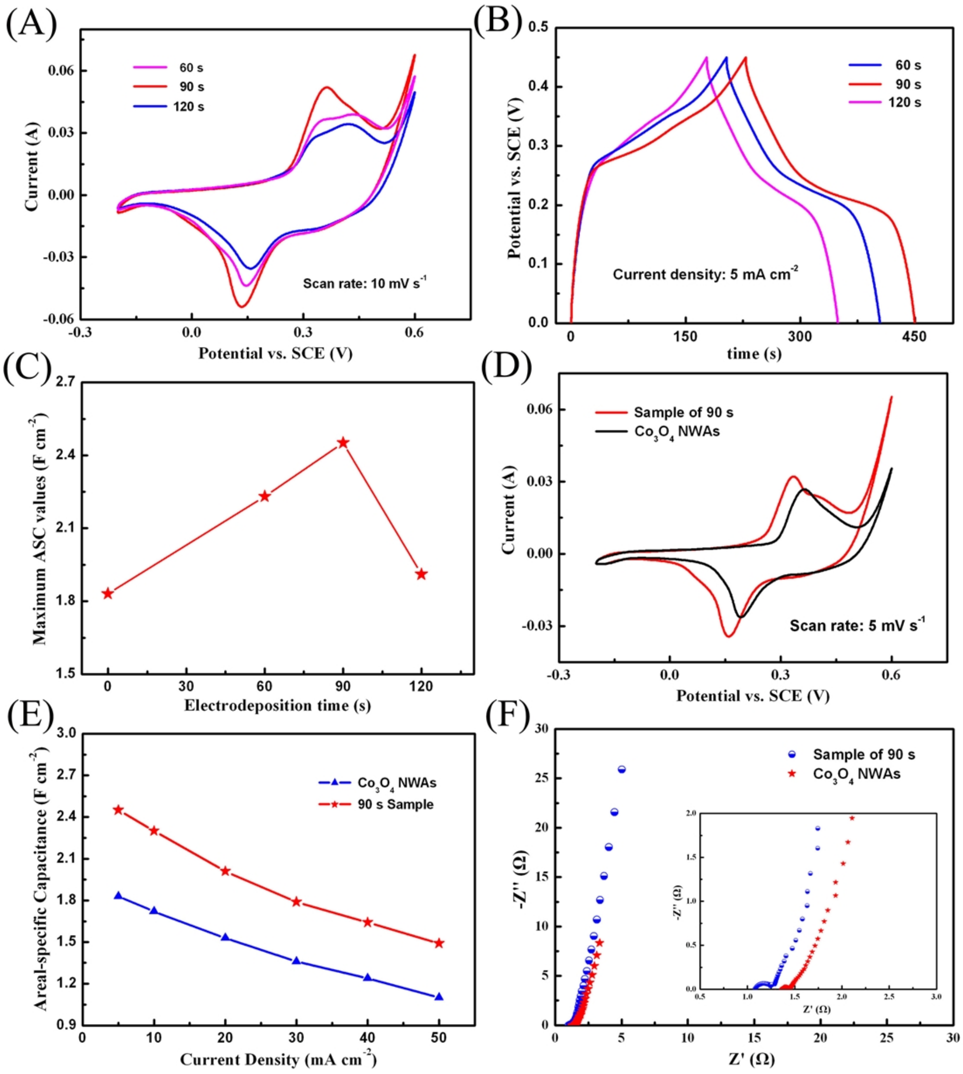

Fig. S5 (A) CV curves of the Co_3O_4@PPy NWAs electrodes at a scan rate of 10 mV s^{-1}, (B) Charge/discharge curves of the Co_3O_4@PPy NWAs electrodes at 5 mA cm^{-2}, (C) The maximum ASC values of the Co_3O_4@ PPy NWAs electrodes as a function of deposition time, (D) CV curves of the pristine Co_3O_4 NWAs and Co_3O_4@PPy NWAs electrodes at a scan rate of 5 mV s^{-1}, (E) ASC values of the pristine Co_3O_4 NWAs and hybird Co_3O_4@PPy NWAs electrodes as a function of current densities, (F) EIS tests with the frequency from 0.01 Hz to 100 kHz. The inset shows the magnified high-frequency regions.

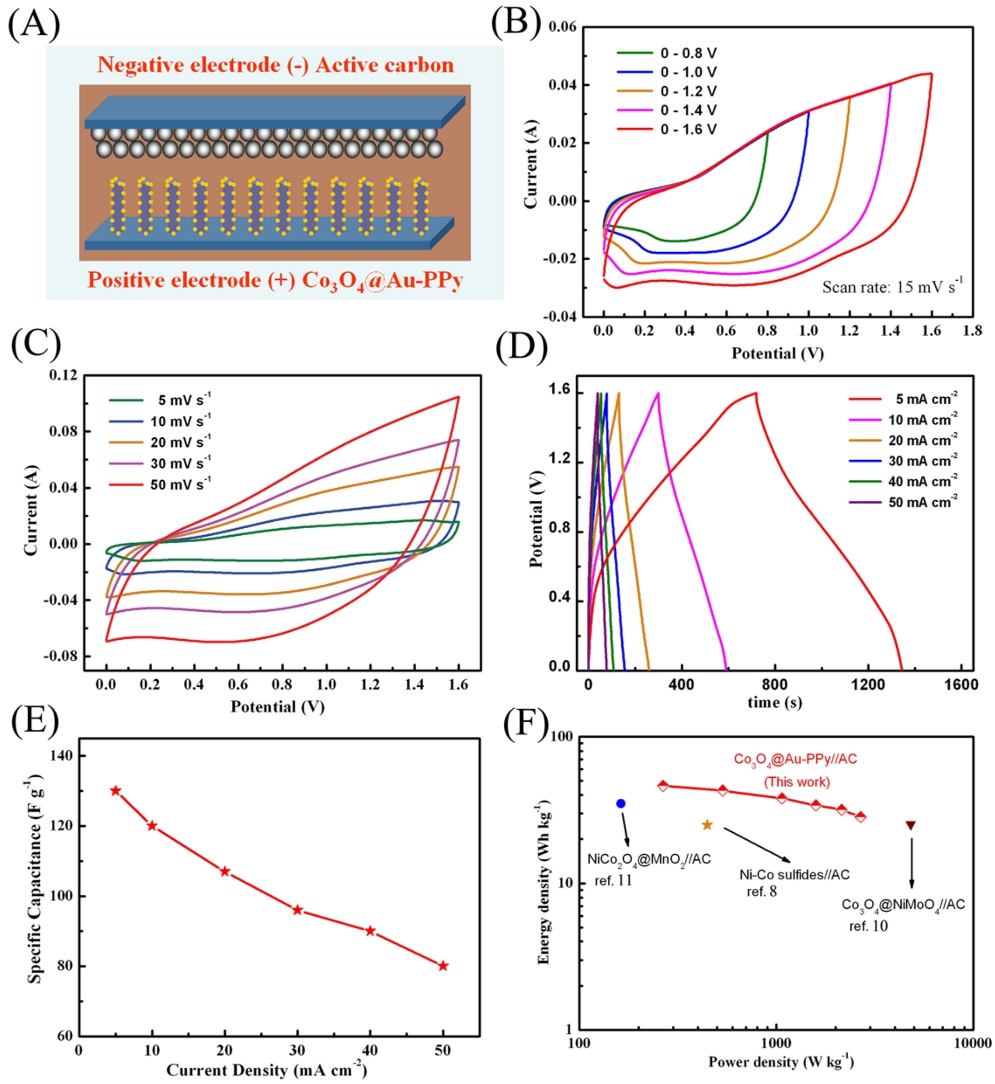

Fig. S6 (A) schematic illustration of the asymmetric supercapacitor configuration, (B, C) CV curves of the as-fabricated Co_3O_4@Au-PPy//AC asymmetric supercapacitor at different scan voltage windows and different scan rates, respectively. (D) charge-discharge curves of the as-fabricated Co_3O_4@Au-PPy//AC asymmetric supercapacitor at different current densities, (E) specific capacitance values of the Co_3O_4@Au-PPy//AC asymmetric supercapacitor as function of current density, (F) Ragone plot of the Co_3O_4@Au-PPy//AC asymmetric supercapacitor compared with other reported data.

References

1. C. Guan, Z. Zeng, X. Li, X. Cao, Y. Fan, X. Xia, G. Pan, H. Zhang and H. J. Fan, *Small*, 2014, **10**, 300-307.
2. X. H. Xia, J. Tu, Y. Zhang, J. Chen, X. Wang, C. Gu, C. Guan, J. Luo and H. J. Fan, *Chem. Mater.*, 2012, **24**, 3793-3799.
3. (a) X. H. Xia, J. P. Tu, Y. Q. Zhang, X. L. Wang, C. D. Gu, X. B. Zhao and H. J. Fan, *ACS Nano*, 2012, **6**, 5531-5538; (b) X. H. Xia, J. P. Tu, Y. Q. Zhang, Y. J. Mai, X. L. Wang, C. D. Gu and X. B. Zhao, *RSC Adv.*, 2014, **2**, 1835-1841.
4. C. Zhou, Y. Zhang, Y. Li and J. Liu, *Nano lett.*, 2013, **13**, 2078-2085.
5. B. Wang, X. Y. He, H. P. Li, Q. Liu, J. Wang, L. Yu, H. J. Yan, Z. S. Li and P. Wang, *J. Mater. Chem. A*, 2014, **2**, 12968-12973.
6. L. Han, P. Tang and L. Zhang, *Nano Energy*, 2014, **7**, 42-51.
7. J. Hu, K. Xu, R. Zou, X. Huang, W. Li, Q. Liu, X. Liu, S. Li and J. Yang, *J. Mater. Chem. A*, 2014, **2**, 16731-16739.
8. Y. Li, L. Cao, L. Qiao, M. Zhou, Y. Yang, P. Xiao and Y. Zhang, *J. Mater. Chem. A*, 2014, **2**, 6540-6548.
9. H. Chen, L. Hu, M. Chen, Y. Yan and L. Wu, *Adv. Funct. Mater.*, 2014, **24**, 934-942.
10. W. Hong, J. Wang, P. Gong, J. Sun, L. Niu, Z. Yang, Z. Wang and S. Yang, *J. Power Sources*, 2014, **270**, 516-525.
11. K. Xu, W. Li, Q. Liu, B. Li, X. Liu, L. An, Z. Chen, R. Zou and J. Hu, *J. Mater. Chem. A*, 2014, **2**, 4795-4802.